Kinetic Analysis of the Endonuclease Activity of Phage λ Terminase: Assembly of a Catalytically Competent Nicking Complex Is Rate-Limiting†

Liping Woods,‡ Christopher Terpening,‡ and Carlos Enrique Catalano*,‡,§

Department of Pharmaceutical Sciences, School of Pharmacy, and Molecular Biology Program, School of Medicine, University of Colorado Health Sciences Center, Denver, Colorado 80262

Received December 11, 1996; Revised Manuscript Received February 13, 1997⊗

ABSTRACT: The terminase enzyme from bacteriophage λ is responsible for excision of a single genome from a concatameric DNA precursor and its insertion into an empty viral procapsid. The enzyme possesses a site-specific endonuclease activity which is responsible for excision of the viral genome and the formation of the 12 base-pair single-stranded "sticky" ends of mature λ DNA. We have previously reported a kinetic analysis of the endonuclease activity of λ terminase which showed an enzyme concentration-dependent change in the kinetic time course of the reaction [Tomka, M. A., & Catalano, C. E. (1993b) *J. Biol. Chem. 268*, 3056−3065]. We presented a model which suggested that the rate-limiting step in the nuclease reaction was the assembly of a catalytically competent prenicking complex. Here, we provide additional evidence for a slow assembly step in the nuclease reaction and demonstrate that the observed rate is affected by protein concentration, but not by the length of the DNA substrate. Consistent with our model, preincubation of terminase with DNA also yields an observable fast phase of the reaction, but only when large (≥3 kb) DNA substrates are used. Finally, we present data which demonstrate that phage λ terminase can efficiently utilize DNA from the closely related phage ø21 as an endonuclease substrate and that the enzyme binds efficiently to the *cosB* region of both phage genomes. The implications of these results with respect to the assembly of a catalytically competent nucleoprotein complex required to initiate genome packaging are discussed.

Assembly of an infectious virus proceeds through an ordered sequence of nucleoprotein intermediates derived from both virus and host gene products (Black, 1989; Casjens, 1985; Earnshaw & Casjens, 1980). In the case of bacteriophage λ, the virus is assembled from pre-formed viral capsids, or proheads, tails, and full-length genomes, which are excised from a concatameric DNA precursor (Catalano et al., 1995; Feiss & Becker, 1983; Murialdo, 1991). Cutting of a single genome (mature DNA) from the concatamer (immature DNA) and its insertion into the empty prohead is the responsibility of the terminase enzyme (Becker & Murialdo, 1990; Catalano et al., 1995; Feiss, 1986). λ terminase is composed of the phage gene products gpA[1] (72 kDa) and gpNu1 (20.4 kDa), and the holoenzyme (gpA_1·$gpNu1_2$) has been shown to possess site-specific endonuclease (Higgins et al., 1988; Rubinchik et al., 1994b; Tomka & Catalano, 1993b), ATPase (Hwang et al., 1995; Rubinchik et al., 1994a; Tomka & Catalano, 1993a), and helicase (Higgins et al., 1988; Parris et al., 1994) catalytic activities. These activities work in concert to excise a single genome from the concatamer and package it within the confines of the viral capsid. The packaging process initiates with the assembly of the terminase subunits at the cohesive end site (*cos*) of λ DNA, the junction between individual genomes in the concatamer, and symmetric nicking of the duplex 12 bases apart (the TER reaction, Figure 1) (Becker & Murialdo, 1990; Catalano et al., 1995; Feiss, 1986). *Escherichia coli* integration host factor (IHF) has been shown to stimulate the TER reaction, presumably by promoting cooperative binding of gpA and gpNu1 at *cos* (Gold & Parris, 1986; Shinder & Gold, 1989; Tomka & Catalano, 1993b). Terminase-mediated strand separation yields complex I, the first stable intermediate in the packaging pathway (Becker et al., 1977). This binary enzyme·DNA intermediate ($T{\cdot}D_L$, Figure 1) is composed of the protein subunits bound to the mature left end of the λ genome (Becker et al., 1977; Catalano & Tomka, 1995; Tomka & Catalano, 1993b; Yang et al., 1997). Complex I then binds an empty prohead, which triggers an ATP-dependent terminase translocation along the duplex, and active DNA packaging ensues.[2] Upon encountering the next downstream *cos* site, terminase again introduces staggered nicks and strand separation releases the fully packaged genome (Becker & Murialdo, 1990; Catalano et al., 1995; Feiss, 1986). Similar packaging pathways are used by all of the double-stranded DNA phages as well as the eucaryotic herpes virus groups (Black, 1988; Roizman & Sears, 1991).

The structure of *cos* is tripartite and consists of *cosQ*, *cosN*, and *cosB* (Becker & Murialdo, 1990; Catalano et al., 1995;

† This work was supported by National Science Foundation Grant DMB-9018767 and National Institutes of Health Grant GM50328-02.

* Address correspondence to this author.

‡ Department of Pharmaceutical Sciences.

§ Molecular Biology Program.

⊗ Abstract published in *Advance ACS Abstracts,* April 15, 1997.

[1] Abbreviations: β-ME, 2-mercaptoethanol; *cos*, cohesive end site, the junction between individual genomes in immature concatemeric λ DNA; gpA, large subunit of phage λ terminase; gpNu1, small subunit of phage λ terminase; IHF, *Escherichia coli* integration host factor; kb, kilobase; gp1, small subunit of phage ø21 terminase; gp2, large subunit of phage ø21 terminase; PAGE, polyacrylamide gel electrophoresis; TER reaction, endonuclease activity of the terminase enzyme.

[2] Currently accepted models for terminase-mediated DNA packaging assume that the terminase subunits are part of the translocating complex and likely form the DNA packaging "machine". There is, however, no direct evidence for participation of either of the terminase subunits in this process.

S0006-2960(96)03044-9 CCC: $14.00

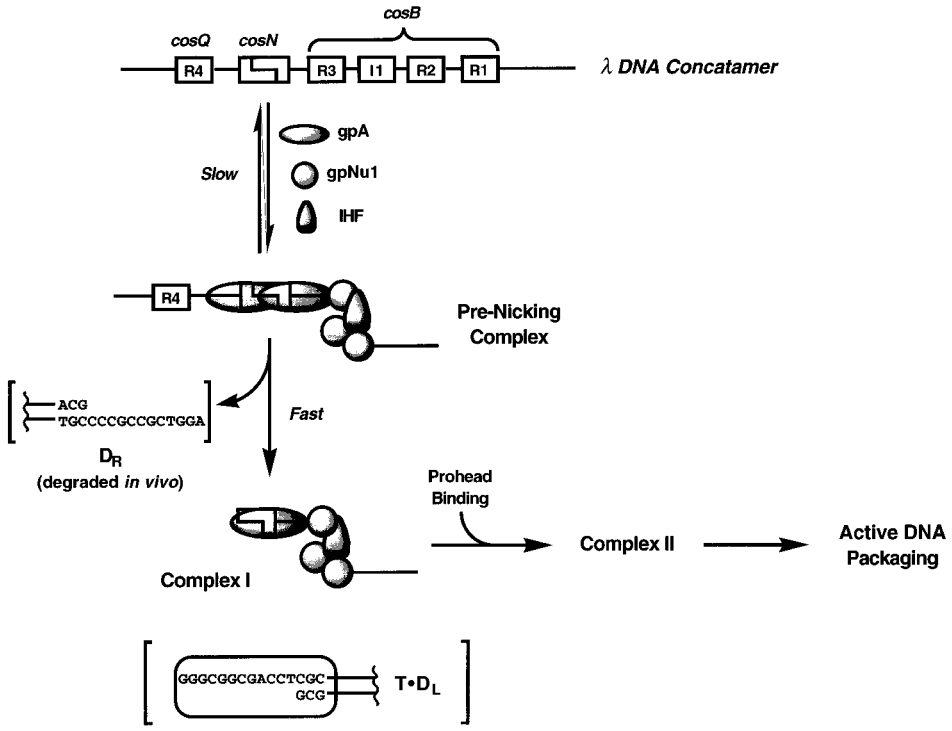

FIGURE 1: Proposed model for *cos*-cleavage by λ terminase. The elements which make up the *cos* sequence of the λ genome are shown at the top of the figure. Assembly of a prenicking complex at the concatameric *cos* site is the first step in the *cos*-cleavage reaction. Once assembled, the gpA subunit of the enzyme introduces symmetric nicks within *cosN* and subsequent strand separation (helicase activity) releases D_R thus forming complex I ($T{\cdot}D_L$). The sequence of the strand-separated "sticky" ends of the phage λ genome are indicated in brackets. Complex II is formed upon binding of an empty prohead to complex I and DNA packaging ensues. At low enzyme concentrations, the rate of *cos*-cleavage is limited by the rate of prenicking complex assembly. As the concentration of terminase is increased, the assembly step becomes faster and ultimately a change in the rate-limiting step of the reaction is observed. Details of the mechanism are discussed in the text.

Feiss, 1986) (Figure 1). The *cosQ* element is upstream from *cosN* and plays an important role in the terminal *cos*-cleavage reaction which occurs subsequent to genome packaging (Cue & Feiss, 1992a, 1993b). The 16 bp sequence of *cosN* shows 2-fold rotational symmetry, and the nicks introduced by terminase fall within this element (Feiss & Becker, 1983; Higgins et al., 1988). Under certain conditions, the isolated terminase gpA subunit possesses endonuclease activity (Rubinchik et al., 1994b), and it has been suggested that assembly of a gpA dimer symmetrically disposed at *cosN* is required for duplex nicking (Becker & Murialdo, 1990; Catalano et al., 1995; Murialdo, 1991). Efficient nuclease activity requires the presence of the gpNu1 subunit, however (Rubinchik et al., 1994b; C. E. Catalano, unpublished results). Genetic (Cue & Feiss, 1992b, 1993a; Feiss et al., 1983) and biochemical (Shinder & Gold, 1988, 1989) studies have demonstrated that gpNu1 binds to three consensus sequences (R3-R2-R1) found within the ~150 bp *cosB* region, and current models suggest that cooperative assembly of gpNu1 at the individual R elements is required for efficient binding of gpA at *cosN* (Becker & Murialdo, 1990; Catalano et al., 1995; Murialdo, 1991). An IHF-binding site has also been identified within *cosB*, and gel retardation (Kosturko et al., 1989; C. E. Catalano, unpublished results) and DNase footprinting (Shinder & Gold, 1989; Xin & Feiss, 1988, 1993) studies have shown direct interactions of IHF with *cosB*. The assembly of a catalytically competent nicking complex at *cos* thus requires cooperative binding interactions of IHF, gpNu1, and gpA across multiple elements within the *cos* region of the λ genome. Moreover, ATP (but not ATP hydrolysis) has also been shown to affect the rate and fidelity of the endonuclease activity of the enzyme (Cue & Feiss, 1993a; Higgins & Becker, 1994; Higgins et al., 1988).

Bacteriophage ø21 is a lambdoid phage closely related to λ (Feiss & Becker, 1983). The viruses possess 64% sequence identity across their *cos* sequences (Miller & Feiss, 1985); they nevertheless display remarkable specificity in genome packaging with phage λ terminase packaging only λ DNA into λ proheads (Feiss et al., 1981; Hohn, 1975). Similarly, phage ø21 terminase, composed of analogous large (gp2) and small (gp1) subunits, packages only phage ø21 DNA within phage ø21 proheads (Feiss et al., 1979, 1981). The *cosN* sequences of the two viruses are identical and are functionally homologous (Feiss & Widner, 1982; Miller & Feiss, 1985). It is thus expected that no discrimination in genome packaging may be derived from direct gpA·*cosN* (or gp2·*cosN*) binding interactions. Both viral genomes possess a *cosB* region containing an IHF-binding site and three R elements in the same relative positions (Feiss & Becker, 1983; Miller & Feiss, 1985) (see Figure 1). The R element consensus sequences differ between the phage, however, and it has been suggested that packaging specificity is driven by the terminase small subunits (gpNu1 and gp1 for λ and ø21, respectively) binding to their respective R elements in *cosB* (Feiss et al., 1981).

Our laboratory has previously reported a kinetic analysis of the phage λ TER reaction which demonstrated that (1) the reaction corresponded to a single enzyme turnover, presumably due to the formation of complex I and (2) the reaction time course was complex and varied with the concentration of enzyme included in the reaction mixture (Tomka & Catalano, 1993b). We suggested that the biphasic

kinetics observed at elevated enzyme concentrations were due to a slow assembly step (k_{slow}) which was required for the formation of a catalytically competent nicking complex followed by rapid duplex nicking (k_{fast}) (Figure 1). We present experiments here which further suggest that assembly of the terminase subunits at *cos* is indeed rate-limiting in *cos*-cleavage. Moreover, the effects of DNA length on this putative rate-limiting step are examined. Finally, we demonstrate that the terminase enzyme from bacteriophage λ can efficiently utilize phage ø21 *cos*-containing DNA as an endonuclease substrate and directly demonstrate that the λ terminase gpNu1 subunit efficiently binds to the *cosB* region of the phage ø21 genome.

EXPERIMENTAL PROCEDURES

Materials and Methods. Tryptone, yeast extract, and agar were purchased from DIFCO. Restriction enzymes, calf intestinal alkaline phosphatase, bacteriophage T4 polynucleotide kinase, bacteriophage T4 ligase, and the plasmid pGEM9Zf(−) were purchased from Promega. Unlabeled nucleoside triphosphates and ampicillin were purchased from Sigma Chemical Co. Radionucleotides were purchased from ICN. All other materials were of the highest quality commercially available.

Bacterial Strains and Protein Purification. The plasmids pSF1 and pAFP1 which contain the entire wild-type *cos* sequence (*cosQ-cosN-cosB*) from phage λ cloned into pBR322 (Feiss et al., 1981) and pUC19 (Cue & Feiss, 1992a) backgrounds, respectively, were purified from *E. coli* strains C600[pSF1] and JM107[pAFP1]. The plasmid pBW3, which contains the entire wild-type *cos* sequence from phage ø21 cloned into a pBR322 background (Feiss & Widner, 1982), was purified from *E. coli* strain IC202[pBW3]. The above strains were a generous gift of M. Feiss (University of Iowa, Iowa City, IA).

Phage λ terminase was purified from AZ1930 (generously provided by H. Murialdo, University of Toronto, Toronto, Ontario, Canada) as described by Tomka and Catalano (1993b). The isolated terminase subunits, gpNu1 and gpA, were purified as described by Hanagan et al. [Hanagan, A., Meyer, J. D., Manning, M. C., & Catalano, C. E. (manuscript in preparation)]. The concentration of catalytically active terminase (holoenzyme and reconstituted enzyme) was determined by active-site titration experiments (Tomka & Catalano, 1993b). *E. coli* integration host factor was purified from HN880 (a kind gift of H. Nash, National Institutes of Health, Bethesda, MD) by the method of Nash et al. (1987). All of our purified proteins were homogeneous as determined by SDS-PAGE and densitometric analysis using a Molecular Dynamics laser densitometer and the ImageQuant data analysis package. Unless otherwise indicated, protein concentrations were determined by BCA assay (Dunn, 1994).

Construction of pCT-λ and pCT-21. The plasmids pSF1 (phage λ *cos*) and pBW3 (phage ø21 *cos*) were digested with *Eco*RI−*Sal*I (double digest) and *Hin*dIII, respectively, and the *cos*-containing fragments were fractionated on an 0.8% agarose gel. The appropriate bands were excised from the gel and purified using the Qiaex II kit according to the manufacturer's instructions. The plasmid pGEM9Zf(−) was similarly digested, and the vectors were dephosphorylated with calf intestinal alkaline phosphatase. The *cos*-containing inserts were then ligated into the appropriately digested vector using T4 ligase and used to transform *E. coli* DH5α cells. Colonies were selected from ampicillin-containing LB plates, plasmids were isolated from overnight cultures, and the presence of the appropriate insert was verified by restriction enzyme digestion.

Table 1: DNA Substrates Used in This Study[a]

DNA substrate	*cos*-sequence	size (kb)
266mer	phage λ	0.266
pAFP1	phage λ	2.9
pCT-λ	phage λ	12
348mer	phage ø21	0.348
pCT-21	phage ø21	10
NS−DNA	none (nonspecific sequence)	0.216

[a] Each of the DNA substrates contains the entire *cos*-sequence (*cosQ-cosN-cosB*, Figure 1) from the indicated phage genome cloned into a plasmid background. The construction of each of the DNA substrates is described in Experimental Procedures.

Preparation of cos-Cleavage DNA Substrates. The DNA substrates used in these studies are described in Table 1. All plasmid purifications utilized Qiagen DNA prep columns according to the manufacturers' instructions. Linearization of the phage λ *cos*-containing substrates used in these studies was accomplished by digestion of pAFP1 (3 kb) and pCT-λ (12 kb) with *Sca*I and *Sal*I, respectively, according to the manufacturer's recommendations. Preparation of the phage ø21 *cos*-containing substrate was similarly performed by linearization of pCT-21 (10 kb) with *Sca*I. The 266 bp phage λ *cos*-containing substrate (266mer, Table 1) was obtained by *Eco*RI−*Hin*dIII double-digestion of pAFP1 and purification of the fragment by 1% agarose gel using standard methods (Maniatis et al., 1982). A 348 bp phage ø21 *cos*-containing substrate was similarly prepared by double-digestion of pCT-21 with *Sac*II and *Bsp*M1 and purification as described above. A 216 bp nonspecific (*cos*-minus) DNA substrate was also prepared by double digestion of pAFP1 with *Eco*RI and *Nde*I. In all cases, the gel-purified DNA fragments were phenol−chloroform extracted and precipitated with ethanol, and the washed pellet was taken into TE buffer. The final concentrations of DNA were determined by UV spectroscopy (Maniatis et al., 1982) using a Hewlett-Packard HP8452A spectrophotometer. Labeling at the 5′ and 3′ ends of the DNA substrates utilized T4 polynucleotide kinase and [γ^{32}P]ATP and the Klenow fragment and [α^{32}P]-dATP, respectively, according to standard methods (Maniatis et al., 1982).

Endonuclease (cos-Cleavage) Assays. The *cos*-cleavage assays (25 μL) contained 20 mM Tris buffer (pH 8), 10 mM $MgCl_2$, 2 mM spermidine, 7 mM β-ME, and 1 mM ATP. Unless otherwise stated, the indicated DNA substrate was included at a concentration of 200 nM with an equalimolar concentration of IHF. The reaction was initiated with the addition of terminase holoenzyme (200 nM, unless otherwise stated), and the reaction was allowed to proceed at 37 °C. Aliquots (3 μL) were removed at the indicated times, and the reaction was stopped with the addition of an equal volume of 100 mM EDTA. For the larger substrates, the DNA was fractionated by 0.6% agarose gel and the ethidium bromide-stained products were analyzed by video densitometry as previously described (Tomka & Catalano, 1993b). For the smaller (∼250−350 bp) substrates, the ^{32}P-end-labeled products were fractionated by 8% PAGE and analyzed using a Molecular Dynamics personal phosphorimager. In all cases, the raw data were quantitated using the Molecular Dynamics ImageQuant software package.

Kinetic Analysis. Each data set was analyzed according to both eqs 1 and 2, which describe monophasic and biphasic reaction time courses, respectively:

$$\text{products} = A - B\exp(-k_1\tau) \quad (1)$$

$$\text{products} = A - B\exp(-k_1\tau) - C\exp(-k_2\tau) \quad (2)$$

where products refers to the fraction of DNA digested at time τ and A is the extent of the reaction at $\tau = \infty$. B and C describe the fraction of the observed rate associated with the slow and fast phases, respectively, and k_1 and k_2 represent the observed rate constants for the slow phase (k_{slow}) and fast phase (k_{fast}) of the reaction, respectively. The indicated constants were determined by nonlinear regression analysis of the experimental data using the Igor data analysis program (Wave Metrics, Lake Oswego, OR) as described previously (Tomka & Catalano, 1993b). A monoexponential curve function was deemed appropriate to describe the data if (1) the values of the rate constants, k_1 and k_2, obtained by nonlinear regression analysis of the data to eq 2 differed by less than 10-fold *and* (2) the ψ^2 value obtained from fitting to eq 1 was within an order of magnitude of that obtained from fitting to eq 2.

Gel Mobility Shift Experiments. Unless otherwise indicated, the binding buffer used in these studies was 20 mM Tris (pH 8) containing 1 mM ATP, 5 mM spermidine, 1 mM EDTA, 7 mM β-ME, and 10% glycerol. The ^{32}P-end-labeled DNA substrates were included at a concentration of 1 nM, and gpNu1 was added at the indicated concentrations. The mixtures (10 μL) were kept at room temperature for 20 min and then loaded (neat) onto a 5% polyacrylamide gel (acrylamide:bisacrylamide ratio of 80:1). The gels were run in 0.5 × TBE at 10 V/cm for 2 h and dried onto Whatmann 3MM filter paper and the dried gels analyzed using a Molecular Dynamics personal phosphorimager and the ImageQuant software package. The raw data were fit to the following logistical sigmoidal curve function:

$$\text{fraction free DNA} = \frac{(m_x + b_x) - (m_n + b_n)}{1 + \left(\frac{[\text{protein}]}{C_{1/2}}\right)^{m_s}} + m_n + b_n \quad (3)$$

where m_x/m_n and b_x/b_n represent the slopes and y-intercepts of the maximum and minimum baselines, respectively, m_s represents the slope of the curve within the transition region, and $C_{1/2}$ represents the midpoint (inflection point) of the curve. The indicated constants were determined by nonlinear regression analysis of the experimental data using the Igor data analysis program (Wave Metrics) as described previously (Yang et al., 1997). $C_{1/2}$ mathematically represents the concentration of protein required to half-deplete free DNA and thus provides a crude approximation of the relative binding affinities of proteins for DNA (Carey, 1991). In all cases where $C_{1/2}$ was determined using the above equations, the concentration of DNA was less than 0.2% of the calculated protein concentration.

RESULTS

Both of the Terminase Subunits Are Required for Efficient cos-Cleavage. Genetic (Davidson & Gold, 1992; Wong & Feiss, 1996) and biochemical (Rubinchik et al., 1994b) experiments have demonstrated that the endonuclease activity of the terminase enzyme is located within the gpA subunit. Table 2 shows, however, that neither the gpNu1 nor the gpA subunit individually possess any detectable *cos*-cleavage activity under the experimental conditions utilized here. Reconstitution of the terminase enzyme from the isolated subunits restores endonuclease activity to wild-type levels, a result similar to that reported by Rubinchik et al. (1994b).[3] While the *cosN* region of the phage ø21 genome is identical to that of phage λ, the *cosB* regions differ and it has been suggested that gpNu1 might not interact significantly with the *cosB* region of the phage ø21 genome (Feiss et al., 1981). This suggestion has been supported by *in vitro cos*-cleavage experiments which demonstrated that λ terminase cuts phage ø21 *cos*-containing DNA at ~1% the efficiency of a λ *cos*-containing substrate (Feiss et al., 1981; Kobayashi et al., 1984). We show here, however, that gpNu1 also stimulated gpA-mediated cleavage of pCT-21, a phage ø21 *cos*-containing DNA substrate (Table 2). Figure 2 similarly demonstrates that phage λ terminase can efficiently utilize a phage ø21 *cos*-containing DNA substrate, albeit at elevated protein concentrations. These data suggest that (1) gpNu1 stimulates gpA binding to *cosN* by direct protein·protein interactions and/or (2) the phage λ gpNu1 protein binds to the *cosB* region of the phage ø21 genome.

Table 2: Endonuclease Activity of the Terminase gpA Subunit Is Dependent upon gpNu1[a]

DNA substrate	gpA	gpNu1	% DNA cut
pCT-λ	−	+	ND[b]
pCT-λ	+	−	ND[b]
pCT-λ	+	+	30
pCT-21	−	+	ND[b]
pCT-21	+	−	ND[b]
pCT-21	+	+	4

[a] The terminase gpA and gpNu1 subunits were added to 200 and 400 nM, respectively, as indicated in the table, and the amount of DNA cut in 60 min was analyzed by gel assay as described in Experimental Procedures. The linearized DNA substrates pCT-λ and pCT-21, which contain the *cos* sequences from phage λ and ø21, respectively (Table 1), were included at 200 nM. [b] ND, no nuclease activity (<1%) was detected by gel assay.

Kinetics of the cos-Cleavage Reaction. We have previously characterized the *cos*-cleavage activity of λ terminase and have reported that the time course of the reaction varied with the reaction conditions (Tomka & Catalano, 1993b). At low enzyme concentrations, the time course was best described by a single-exponential curve function and was consistent with a single rate-limiting step. As the concentration of enzyme was increased, however, the time course became biphasic with a second, faster phase appearing in the rate profile. This experiment is reproduced in Figure 3 (panel A), and the kinetic rate constants derived from these data (Table 3) are quite consistent with those reported earlier [$k_{slow} = 0.058$ min^{-1}, $k_{fast} = 0.464$ min^{-1} (Tomka & Catalano, 1993b)]. Note that at elevated enzyme concentrations a fast

[3] Gold and co-workers have demonstrated that the isolated gpA subunit could under certain experimental conditions cut *cos*-containing DNA (Rubinchik et al., 1994b). While we have similarly observed gpA-mediated *cos*-cleavage, the concentration of gpA required was 10-fold greater than that utilized in these studies and the reaction conditions were different from those used here, conditions which Gold and co-workers describe as optimal, but "nonspecific" *cos*-cleavage conditions (Rubinchik et al., 1994b).

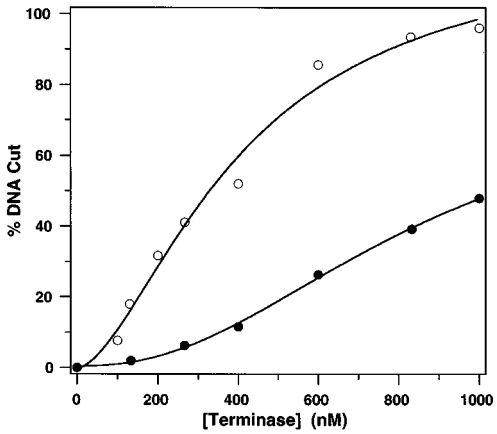

FIGURE 2: λ terminase utilizes both phage λ and phage ø21 DNA as a *cos*-cleavage substrate. Linearized pCT-λ (○) or pCT-21 (●) was used as a DNA substrate in the *cos*-cleavage reaction as described in Experimental Procedures. λ terminase was added as indicated, and the amount of DNA cut in 60 min was determined by gel assay. Each data point represents the average of three separate experiments.

rate appears which is roughly an order of magnitude greater than the slow phase of the reaction curve. The DNA substrate used in this and prior experiments was a phage λ *cos*-containing plasmid ~3 kb in length. Figure 3 demonstrates that virtually identical results were obtained using larger (12 kb, panel B) and smaller (0.266 kb, panel C) phage λ *cos*-containing DNA substrates. Moreover, analysis of the data yielded slow and fast rate constants quite similar to those obtained with the 3 kb substrates (Table 3). Unlike the phage λ *cos*-containing DNA substrates, λ terminase-mediated cleavage of a phage ø21 *cos*-containing DNA substrate (pCT-21) yielded monophasic kinetics under all enzyme concentrations examined (Figure 3D). Analysis of the data suggests that only the slow phase of the reaction curve is observed when pCT-21 is used as a *cos*-cleavage DNA substrate (Table 3).

Table 3: Enzyme Concentration Affects *cos*-Cleavage Kinetics[a]

DNA substrate	substrate size (kb)	[terminase] (nM)	k_{slow} (min^{-1})	k_{fast} (min^{-1})
pAFP1	2.9	200	0.0439	*b*
pAFP1	2.9	800	0.0124	0.214
pCT-λ	12	200	0.0054	*b*
pCT-λ	12	800	0.0150	0.427
266mer	0.266	200	0.0182	*b*
266mer	0.266	800	0.0499	0.482
pCT-21	10	800	0.0054	*b*
pCT-21	10	1600	0.0072	*b*

[a] The kinetic rate constants derived from analysis of the data displayed in Figure 3 are presented in the table. Details of the experimental conditions used in each experiment are discussed in the legend to Figure 3. [b] The data were equally well described with a single-exponential curve function by the criteria discussed in Experimental Procedures.

Prenicking Complex Assembly Is the Rate-Limiting Step in cos-Cleavage. We have previously suggested that the unusual kinetics observed in the *cos*-cleavage reaction were due to a slow assembly step which limited the reaction rate at low enzyme concentrations (Tomka & Catalano, 1993b) (Figure 1). This model suggested that as the enzyme concentration was increased, the rate of assembly of a catalyically competent nicking complex at *cos* increased until a second step (or series of steps) became rate-limiting, thus yielding the fast phase of the reaction profile. We reasoned

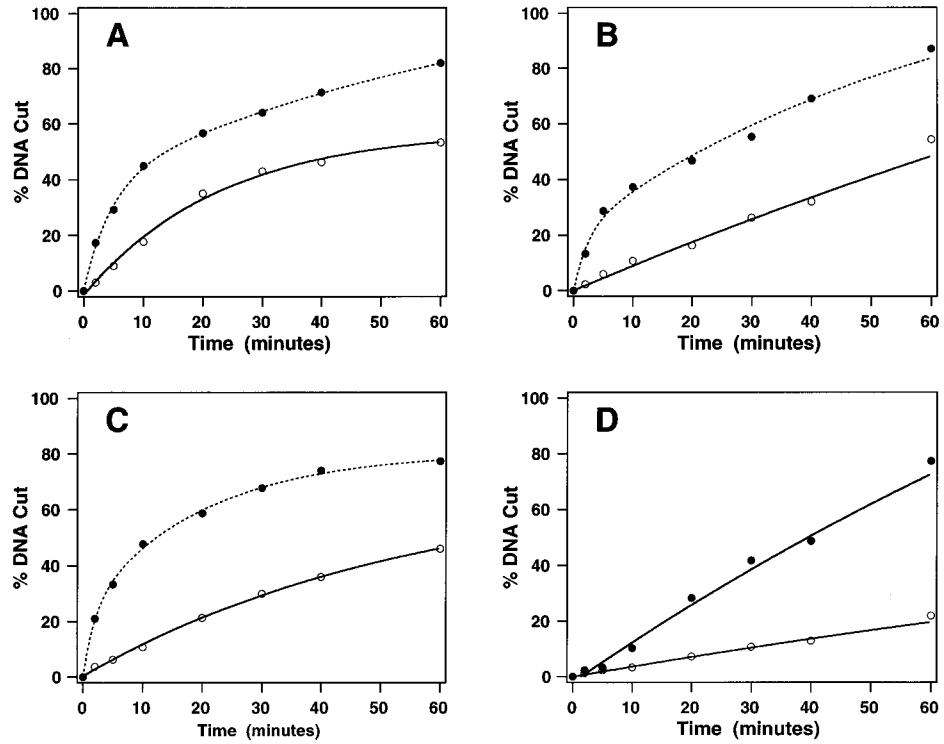

FIGURE 3: *cos*-cleavage kinetics depend upon terminase concentration. Phage λ terminase was added to a reaction mixture containing 200 nM of the indicated linearized DNA substrate as follows (see Table 1). Panel A: pAFP1 DNA in the presence of (○) 200 nM or (●) 800 nM enzyme. Panel B: pCT-λ in the presence of (○) 200 nM or (●) 800 nM enzyme. Panel C: 266_{mer} DNA in the presence of (○) 200 nM or (●) 800 nM enzyme. Panel D: pCT-21 DNA in the presence of (○) 800 nM or (●) 1600 nM enzyme. Each data point represents the average of three separate experiments. The reaction time courses were analyzed as described in Experimental Procedures. The solid lines and dotted lines represent the best fit of the data to single-exponential and double-exponential curve functions, respectively, using eqs 1 and 2 as described. The kinetic rate constants derived from these analyses are presented in Table 3.

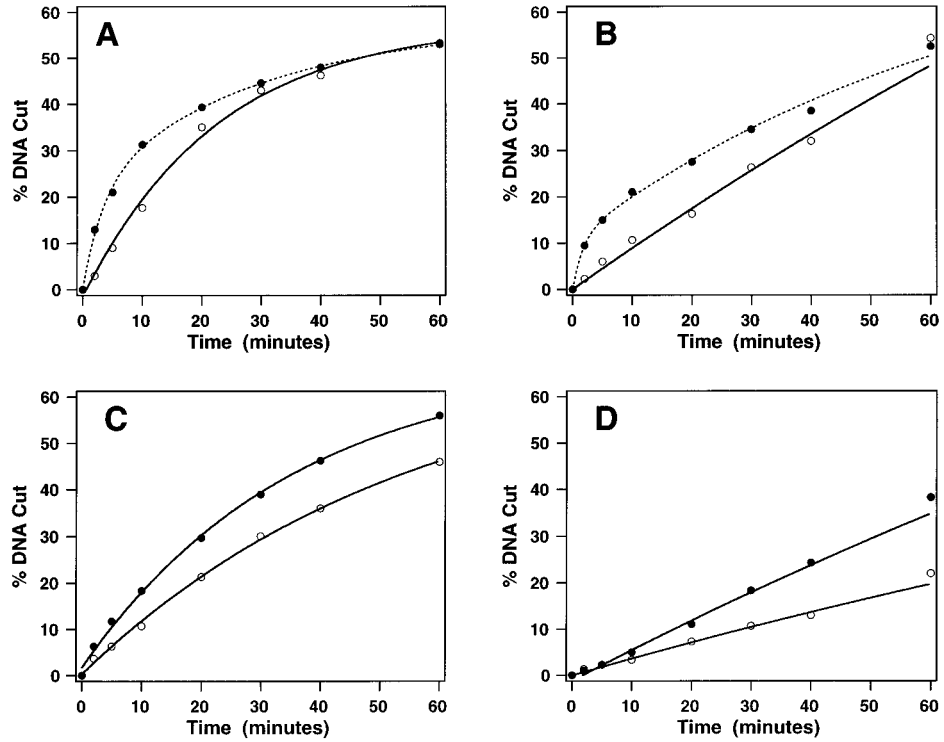

FIGURE 4: Preincubation of enzyme with DNA affects *cos*-cleavage kinetics. The *cos*-cleavage reaction was performed as described in Experimental Procedures except that the DNA substrate was preincubated with either magnesium (○) or phage λ terminase (●) for 15 min at room temperature. The reaction was then initiated with the addition of either enzyme or magnesium, as appropriate, and the nuclease activity analyzed as described. Terminase and DNA were each included to 200 nM in every experiment. The DNA substrates were as follows (see Table 1): panel A, pAFP1; panel B, pCT-λ; panel C, 266_{mer}; panel D, pCT-21. Each data point represents the average of three separate experiments. The solid lines and dotted lines represent the best fit of the data to single-exponential and double-exponential curve functions, respectively, using eqs 1 and 2 as described. The kinetic rate constants derived from these analyses are presented in Table 4.

that preassembly of a nicking complex at *cos* should result in a fast phase of product formation even at low enzyme concentrations. We have previously demonstrated that, while the λ terminase subunits can assemble onto *cos*-containing DNA in the absence of divalent metal (Yang et al., 1997), magnesium (or manganese) is strictly required for the nuclease activity of the enzyme (Tomka & Catalano, 1993b). We thus examined the endonuclease time course subsequent to preincubation of the enzyme (at low concentration) with DNA in the absence of divalent metal. Figure 4 (panel A) demonstrates that preincubation of λ terminase with pAFP1, a 3 kb phage λ *cos*-containing DNA substrate, indeed resulted in a biphasic reaction time course, consistent with a rate-limiting assembly step. Furthermore, Table 4 shows that the rate constants for the slow and fast phases of the reaction profile obtained by preincubating enzyme with DNA were essentially identical to those obtained by using elevated enzyme concentrations (compare Tables 3 and 4). While similar results were obtained with pCT-λ, a 10 kb phage λ *cos*-containing DNA substrate, preincubation of the enzyme with the smaller 0.266 kb phage λ *cos*-containing DNA substrate did not result in a change in the reaction rate profile and simple monophasic kinetics were observed (Figure 4, Table 4). Similarly, preincubation of phage λ terminase with the phage ø21 *cos*-containing DNA substrate did not alter the reaction time course (Figure 4D). In both cases, only the slow phase rate constants were obtained (Table 4).

IHF Stimulates the cos-Cleavage Reaction at Low Enzyme: DNA Ratios. While not strictly required for phage λ replication, *E. coli* integration host factor (IHF) is known to modestly stimulate phage replication *in vivo* (Gold & Parris, 1986). We have previously demonstrated that IHF stimulated

Table 4: Preincubation of Enzyme with DNA Affects *cos*-Cleavage Kinetics[a]

DNA substrate	substrate size (kb)	preincubation mixture	k_{slow} (min^{-1})	k_{fast} (min^{-1})
pAFP1	2.9	minus enzyme	0.0439	*b*
pAFP1	2.9	plus enzyme	0.0341	0.292
pCT-λ	12	minus enzyme	0.0054	*b*
pCT-λ	12	plus enzyme	0.0138	0.588
266mer	0.266	minus enzyme	0.0182	*b*
266mer	0.266	plus enzyme	0.0281	*b*
pCT-21	10	minus enzyme	0.0054	*b*
pCT-21	10	plus enzyme	0.0055	*b*

[a] The kinetic rate constants derived from analysis of the data displayed in Figure 4 are presented in the table. Details of the experimental conditions used in each experiment are discussed in the legend to Figure 4. The preincubation mixtures contained the indicated DNA substrate and either phage λ terminase or magnesium as indicated. [b] The data were equally well described with a single-exponential curve function by the criteria discussed in Experimental Procedures.

the *cos*-cleavage reaction at low terminase concentrations but had little effect at elevated concentrations of the enzyme (Tomka & Catalano, 1993b). These data were consistent with a model suggesting that IHF aided in the cooperative assembly of gpNu1 at the *cosB* region of the λ genome which was in turn required for efficient assembly of gpA at *cosN* and strand nicking (see Figure 1). This experiment was repeated here, and the results presented in Table 5 are identical to those obtained previously: IHF stimulated the *cos*-cleavage reaction ~3-fold, but only at low enzyme concentrations. Virtually identical results were obtained with the 12 kb phage λ *cos*-containing DNA substrate (Table 5). While similar results were also obtained with the 266mer DNA substrate, the effects were more pronounced with a

Table 5: IHF Stimulation of the *cos*-Cleavage Reaction Depends Upon the Terminase Concentration[a]

DNA substrate	substrate size (kb)	terminase concentration (nM)	IHF-mediated stimulation
pAFP1	2.9	200	2.9
pAFP1	2.9	800	1.2
pCT-λ	12	200	2.6
pCT-λ	12	800	1.0
266mer	0.266	200	3.7
266mer	0.266	800	1.7
pCT-21	10	800	2.8
pCT-21	10	1600	1.3

[a] The *cos*-cleavage reaction was performed as described in Experimental Procedures using 200 nM of the indicated DNA substrate in the absence and presence of a stoichiometric concentration of IHF. The reaction was initiated with the addition of terminase holoenzyme at the indicated concentration and the rate of nuclease digestion determined as described. Stimulation was taken as the ratio of the observed rates (k_{obs}) in the presence and absence of IHF[($k_{obs+IHF}$)/($k_{obs-IHF}$)].

nearly 4-fold stimulation at low enzyme concentrations. Moreover, a modest increase in the rate of *cos*-cleavage (~2-fold) was also observed at elevated terminase concentrations (Table 5). Interestingly, the rate of nuclease digestion of pCT-21, the phage ø21 *cos*-containing DNA substrate, showed similar IHF stimulation (Table 5), an unexpected result if the gpNu1 protein does not bind to the *cosB* region of the phage ø21 genome.

The Phage λ Terminase gpNu1 Subunit Binds to Phage ø21 cos-Containing DNA. Phage λ terminase can utilize a phage ø21 *cos*-containing DNA substrate in the *cos*-cleavage reaction (Figure 2), and this reaction is dependent upon the presence of the gpNu1 subunit (Table 2). Moreover, IHF stimulates the reaction (Table 5) and taken together these data suggest that the phage λ gpNu1 protein may bind to the *cosB* region of the phage ø21 genome. We directly examined this possibility using the gel mobility shift assay as described in Experimental Procedures. Figure 5 shows that gpNu1 indeed binds to a phage ø21 *cosB*-containing DNA substrate yielding a single gel retarded complex. The protein concentration dependence of DNA binding is also presented in Figure 5 and demonstrates that gpNu1 does not strongly discriminate between the *cosB* regions of the two phages. Analysis of these data as described in Experimental Procedures yields $C_{1/2}$ values of 1370 ± 340 and 1320 ± 100 nM for phage ø21 and λ *cos*-containing DNA, respectively.

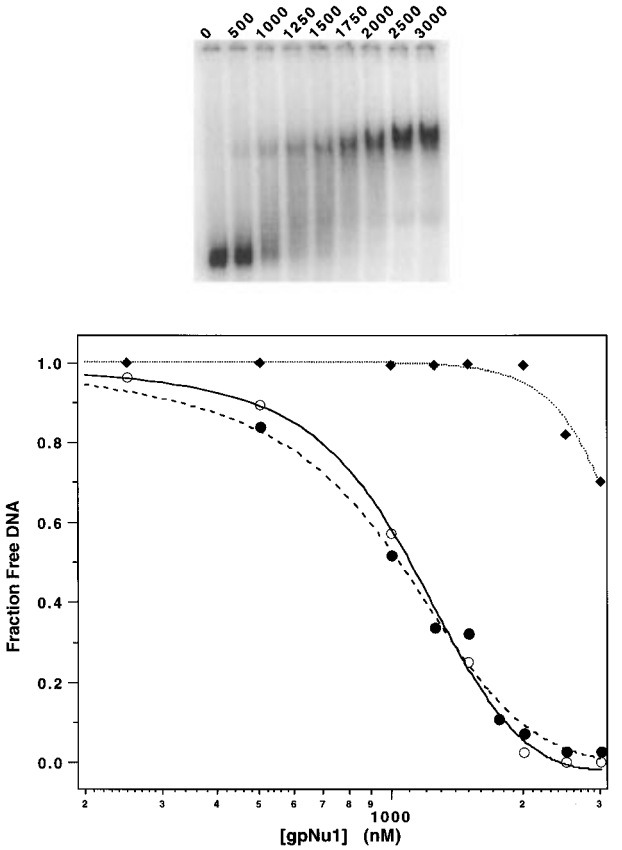

FIGURE 5: The λ terminase gpNu1 subunit binds to *cosB* of phage ø21. Upper panel: phosphor image of the gel retarded complex formed from gpNu1 binding to phage ø21 *cos*-containing DNA (348_{mer}, Table 1). Purified gpNu1 protein was added at the indicated nanomolar concentrations and the protein·DNA complexes were fractionated by ND−PAGE as described in Experimental Procedures. Lower panel: The gel retardation data (performed in triplicate) were analyzed as described, and the fraction of free is DNA shown (●). Also shown in the figure is the analogous experiment performed with a phage λ *cos*-containing DNA fragment (○, 266mer) and a fragment of nonspecific sequence (♦, NS-DNA) (see Table 1). The lines represent the best fit of each data set to eq 3 as described in Experimental Procedures.

DISCUSSION

Terminase enzymes are responsible for genome packaging in all of the double-stranded DNA bacteriophages and in the eucaryotic herpes virus groups (Black, 1989; Roizman & Sears, 1991). The terminase enzyme from bacteriophage λ possesses a site-specific endonuclease catalytic activity which is directly responsible for excision of a single genome from a concatameric DNA precursor and its insertion into an empty viral capsid (Becker & Murialdo, 1990; Catalano et al., 1995; Feiss, 1986). We have previously reported a kinetic analysis of the endonuclease activity of the enzyme (the TER reaction) and presented a model which suggested that assembly of a catalytically competent nicking complex was rate-limiting in the nuclease reaction (Catalano & Tomka, 1995; Tomka & Catalano, 1993b). This model was based upon the fact that at low enzyme concentrations the reaction time course could be adequately described by a single-exponential curve function while at elevated protein concentrations biphasic time courses were observed. This experiment was repeated here with phage λ *cos*-containing DNA substrates of varying length. It is important to note that the entire *cos* sequence (~200 bp) was contained in each of these substrates and only the length was varied. In each case, single-exponential kinetics were observed at low terminase concentrations while biphasic kinetics were observed at elevated enzyme concentrations. Where biphasic kinetics were observed, the rate constant for the fast phase (k_{fast}) was consistently an order of magnitude greater than the rate constant for the slow phase (k_{slow}) of the reaction. Moreover, the rate constants were similar for all of the phage λ *cos*-containing DNA substrates regardless of length. These data are consistent with a model predicting a rate-limiting protein assembly step, as discussed previously, and further suggest that there is little effect of substrate length on the assembly kinetics. Our model is further supported by the fact that IHF stimulates the *cos*-cleavage reaction only when the terminase concentration is low. The putative role of IHF in phage assembly is to stimulate cooperative binding of the gpNu1 subunit(s) at *cosB* which, in turn, stimulates gpA

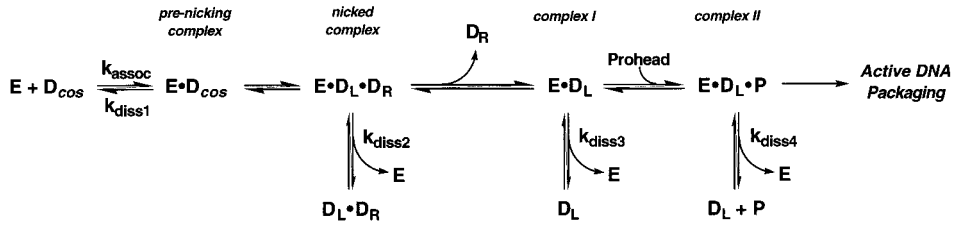

FIGURE 6: Biochemical scheme for fidelity in genome packaging. Packaging of genomic DNA begins with the assembly of terminase holoenzyme (E) at the *cos* site of the λ genome (D_{cos}) forming a binary enzyme·DNA prenicking complex ($E \cdot D_{cos}$). Site-specific nicking at *cosN* yields the nicked, annealed duplex bound to the enzyme ($E \cdot D_L \cdot D_R$). Enzyme-mediated strand separation releases the D_R half-site and generates complex I, terminase bound to the mature left end of the λ genome ($E \cdot D_L$). This stable nucleoprotein intermediate next binds an empty viral prohead forming the ternary enzyme·DNA·prohead complex II ($E \cdot D_L \cdot P$), and active DNA packaging ensues. The stability of each of these nucleoprotein intermediates is critical to productive packaging of the viral chromosome and release of DNA by terminase at any point ($k_{diss1} - k_{diss4}$) would result in aborted packaging. Discrimination in genome packaging may thus result from unstable intermediates formed between phage λ terminase and phage ø21 DNA (or phage ø21 terminase and phage λ DNA) resulting in premature release of DNA and aborted packaging. Details are discussed in the text.

binding to *cosN* and thus increases the rate of DNA strand nicking (Becker & Murialdo, 1990; Catalano et al., 1995; Feiss & Becker, 1983; Murialdo, 1991). Accordingly, IHF should stimulate *cos*-cleavage only when assembly steps are rate-limiting. This prediction is quite consistent with the data presented here, which demonstrate that IHF stimulates terminase-mediated *cos* cleavage 2−3-fold, but only at low enzyme concentrations.

Gel retardation studies performed in our laboratory have previously confirmed that neither of the phage λ terminase subunits requires divalent metal for efficient binding to DNA containing the *cos* site of phage λ (Yang et al., 1997) and protein assembly steps may thus be separated from DNA nicking events. We reasoned that, if assembly were truly rate-limiting at low enzyme concentrations, preincubation of terminase with λ DNA under these conditions should allow nucleoprotein complex assembly and upon addition of Mg^{2+}, a rapid phase of duplex nicking should appear. This prediction was confirmed in experiments presented here. Moreover, the rate constants for the slow and fast phase of the reaction observed when terminase was preincubated with DNA are quite similar to those obtained with elevated enzyme concentrations. These data suggest that the same events are responsible for the biphasic reaction kinetics observed in each case and are fully consistent with a slow, protein concentration-dependent assembly step.

Our data clearly demonstrate biphasic kinetics subsequent to preincubation of terminase with the larger λ DNA substrates; however, the results with the smaller 0.266 kb phage λ *cos*-containing DNA substrate (266mer) are less striking. There is no evidence for a biphasic time course subsequent to preincubation of enzyme with the 266mer. This result contrasts sharply with the protein concentration-dependent appearance of biphasic kinetics using the same small substrate (compare Figures 3 and 4). The above conflicting results suggest that while *assembly* of a catalytically competent nicking complex is rate-limiting for all of the DNA substrates regardless of size, *stability* of the prenicking complex may be impaired with the smaller DNA substrate. In other words, the association rate for the proteins assembling at *cos* (k_{assoc1}, Figure 6) is protein concentration dependent but is not significantly affected by the size of the DNA substrate. The stability of the resultant nucleoprotein complex may depend upon additional "nonspecific" contacts outside of the ~200 bp *cos* sequence, however, which are unavailable with small DNA substrates and the disassembly rate (k_{diss}, Figure 6) is increased. Preincubation of terminase with 266mer DNA may thus form a nucleoprotein complex which dissociates relatively rapidly at the lower enzyme concentrations and does not provide a sufficient concentration of the prenicking complex to yield observable biphasic kinetics. This suggestion is consistent with the observation that IHF does not stimulate *cos*-cleavage at elevated enzyme concentrations when large DNA substrates are used, but modestly stimulates the reaction with the smaller 266 bp substrate.

It has long been appreciated that the terminase enzymes from phage λ and phage ø21 possess genome-specific DNA packaging activities (Feiss et al., 1979, 1981; Hohn, 1975). The *cosB* regions of the viral genomes differ, and it was reasonable to suggest that fidelity in DNA packaging derives from selective binding of the small terminase subunits to their respective R elements within *cosB* (Becker & Murialdo, 1990; Feiss, 1986; Feiss & Becker, 1983; Feiss et al., 1981) (see Figure 1). This model has been supported by *in vitro* *cos*-cleavage experiments which demonstrated that phage λ terminase utilizes ø21 DNA quite poorly (Feiss et al., 1981; Kobayashi et al., 1984). Our data clearly demonstrate, however, that phage λ terminase can efficiently utilize phage ø21 DNA as a *cos*-cleavage substrate. The earlier studies used partially purified enzyme preparations, uninfected *E. coli* extracts, and reaction conditions significantly different than those used in our studies and this may be responsible for the conflicting results. Nevertheless, the requirement for the small terminase subunit and stimulation by IHF suggest that gpNu1·*cosB* interactions are important in the utilization of ø21 DNA as a *cos*-cleavage substrate. These data are inconsistent with a fidelity model based exclusively upon strict selectivity in gpNu1·*cosB* interactions. Moreover, we have directly demonstrated here that the phage λ gpNu1 protein binds efficiently to DNA containing the *cosB* region from either phage. How, then, do we explain the packaging specificity observed *in vivo*?

Multiple terminase·DNA nucleoprotein intermediates are likely formed along the packaging pathway (Figure 6). The stability of each of these nucleoprotein intermediates is critical to efficient viral assembly and premature disassembly of any one (increase in k_{diss}) would lead to aborted packaging. On the basis of studies with mutant gpNu1 terminase enzymes, Cai et al. (1997) have suggested that subtle gpNu1·*cosB* interactions are important not only in the initial interaction of terminase with *cos*, but also in the stability of each of the subsequent packaging intermediates. The gel retardation data presented here demonstrate that the λ

terminase gpNu1 subunit binds efficiently to the *cosB* region of the phage ø21 genome and suggest that the initial interaction with λ and ø21 DNA is not significantly different between the phage. Interestingly, however, while a single gel retarded complex is observed in the interaction of λ terminase with ø21 DNA (see Figure 5), Yang et al. (1997) have observed *three* retarded complexes in the interaction of gpNu1 with *cos*λ-containing DNA. These data suggest that higher order nucleoprotein structures result from specific interactions of gpNu1 with the *cosB* region of the phage λ genome, which are absent with phage ø21 DNA, interactions which may be critical to the stability of subsequent nucleoprotein intermediates. This is consistent with our observation that, while phage λ terminase may efficiently utilize ø21 DNA as a *cos*-cleavage substrate, higher concentrations of enzyme are required, suggesting that binding may, in fact, be slightly altered in the heterologous complex. The observed *in vivo* packaging specificity of phage λ and ø21 may thus derive not from a single protein·DNA recognition event, but rather from an ensemble of nucleoprotein complexes along the packaging pathway, each of which is critical to the packaging process and each of which is important in discrimination between the viral genomes.

ACKNOWLEDGMENT

The authors express their sincere appreciation to Mary Ann Tomka for providing the terminase holoenzyme and Adrienne Hannagan for providing the isolated terminase subunits used in these studies. We are further indebted to Drs. Michael Feiss, Robert Kuchta, and Qin Yang for helpful discussions and for critical review of the manuscript.

REFERENCES

Becker, A., & Murialdo, H. (1990) *J. Bacteriol. 172*, 2819−2824.
Becker, A., Marko, M., & Gold, M. (1977) *Virology 78*, 291−305.
Black, L. W. (1988) DNA Packaging in dsDNA Bacteriophages, in *The Bacteriophages* (Calendar, R., Ed.) pp 321−373, Plenum Publishing Corp., New York.
Black, L. W. (1989) *Annu. Rev. Microbiol. 43*, 267−292.
Cai, A.-H., Hwang, Y., Cue, D., Catalano, C., & Feiss, M. (1997) *J. Bacteriol. 179* (8), 2479−2485.
Carey, J. (1991) *Methods Enzymol. 208*, 103−118.
Casjens, S. R. (1985) An Introduction to Virus Structure and Assembly, in *Virus Structure and Assembly* (Casjens, S. R., Ed.) pp 1−28, Jones and Bartlett Publishers, Inc., Boston, MA.
Catalano, C. E., & Tomka, M. A. (1995) *Biochemistry 34*, 10036−10042.
Catalano, C. E., Cue, D., & Feiss, M. (1995) *Mol. Microbiol. 16*, 1075−1086.
Cue, D., & Feiss, M. (1992a) *J. Mol. Biol. 228*, 58−71.
Cue, D., & Feiss, M. (1992b) *J. Mol. Biol. 228*, 72−87.
Cue, D., & Feiss, M. (1993a) *J. Mol. Biol. 234*, 594−609.
Cue, D., & Feiss, M. (1993b) *Proc. Natl. Acad. Sci. U.S.A. 90*, 9290−9294.
Davidson, A. R., & Gold, M. (1992) *Virology 189*, 21−30.
Dunn, M. J. (1994) Determination of Total Protein Concentration, in *Protein Purification Methods. A Practical Approach* (Harris, E. L. V., & Angal, S., Eds.) pp 10−17, IRL Press, New York.
Earnshaw, W. C., & Casjens, S. R. (1980) *Cell 21*, 319−331.
Feiss, M. (1986) *Trends Genet. 2*, 100−104.
Feiss, M., & Becker, A. (1983) DNA Packaging and Cutting, in *Lambda II* (Hendrix, R. W., Roberts, J. W., Stahl, F. W., & Weisberg, R. A., Eds.) pp 305−330, Cold Spring Harbor Laboratory Press, Plainview, NY.
Feiss, M., & Widner, W. (1982) *Proc. Natl. Acad. Sci. U.S.A. 79*, 3498−3502.
Feiss, M., Fisher, R. A., Siegele, D. A., Nichols, B. P., & Donelson, J. E. (1979) *Virology 92*, 56−67.
Feiss, M., Fisher, R. A., Siegele, D. A., & Widner, W. (1981) Bacteriophage λ and 21 Packaging Specificities, in *Bacteriophage Assembly* (DuBow, M., Ed.) pp 213−222, Alan R. Liss, Inc., New York.
Feiss, M., Widner, W., Miller, G., Johnson, G., & Christiansen, S. (1983) *Gene 24*, 207−218.
Gold, M., & Parris, W. (1986) *Nucleic Acids Res. 14*, 9797−9809.
Higgins, R., & Becker, A. (1994) *EMBO J. 13*, 6152−6161.
Higgins, R. R., Lucko, H. J., & Becker, A. (1988) *Cell 54*, 765−775.
Hohn, B. (1975) *J. Mol. Biol. 98*, 93−106.
Hwang, Y., & Feiss, M. (1996) *J. Mol. Biol. 261*, 524−535.
Hwang, Y., Catalano, C. E., & Feiss, M. (1995) *Biochemistry 35*, 2796−2803.
Kobayashi, I., Stahl, M. M., & Stahl, F. W. (1984) *Cold Spring Harbor Symp. Quant. Biol. 49*, 497−506.
Kosturko, L. D., Daub, E., & Murialdo, H. (1989) *Nucleic Acids Res. 17*, 317−333.
Maniatis, T., Firtsch, E. F., & Sambrook, J. (1982) *Molecular Cloning, A Laboratory Manual*, Cold Spring Harbor Laboratory Press, Plainview, NY.
Miller, G., & Feiss, M. (1985) *J. Mol. Biol. 183*, 246−249.
Murialdo, H. (1991) *Annu. Rev. Biochem. 60*, 125−153.
Nash, H. A., Robertson, C. A., Flamm, E., Weisberg, R. A., & Miller, H. I. (1987) *J. Bacteriol. 169*, 4124−4127.
Parris, W., Rubinchik, S., Yang, Y.-C., & Gold, M. (1994) *J. Biol. Chem. 269*, 13564−13574.
Roizman, B., & Sears, A. E. (1991) Fundamental Virology, in *Fundamental Virology* (Fields, B. N., Knipe, D. M., & Chanock, R. M., Eds.) pp 863−865, Raven Press, New York.
Rubinchik, S., Parris, W., & Gold, M. (1994a) *J. Biol. Chem. 269*, 13586−13593.
Rubinchik, S., Parris, W., & Gold, M. (1994b) *J. Biol. Chem. 269*, 13575−13585.
Shinder, G., & Gold, M. (1988) *J. Virol. 62*, 387−392.
Shinder, G., & Gold, M. (1989) *Nucleic Acids Res. 17*, 2005−2022.
Tomka, M. A., & Catalano, C. E. (1993a) *Biochemistry 32*, 11992−11997.
Tomka, M. A., & Catalano, C. E. (1993b) *J. Biol. Chem. 268*, 3056−3065.
Xin, W., & Feiss, M. (1988) *Nucleic Acids Res. 16*, 2015−2030.
Xin, W., & Feiss, M. (1993) *J. Mol. Biol. 230*, 492−504.
Yang, Q., Hanagan, A., & Catalano, C. E. (1997) *Biochemistry 36*, 2744−2752.

BI963044M